interstellar gas clouds in the manner proposed for the carbon analogue CNC^+.[20] For example, CNC^+ reacts with molecules of the type HX in a manner similar to C^+ to lead to the formation of C–X bonds. Analogous reactions of $CNSi^+$ could lead to Si–X bond formation. The reactions of Si^+ with acetonitrile and cyanoacetylene are possible sources for SiCH and SiC_2 when followed by proton transfer or recombination with electrons as shown:

$$CH_2Si^+ + e(X) \rightarrow SiCH + H(XH^+) \quad (19)$$

$$C_2HSi^+ + e(X) \rightarrow SiC_2 + H(XH^+) \quad (20)$$

Homogeneous association reactions in interstellar gas clouds can proceed only by radiative association because of the low ambient gas densities. The association reactions of atomic Si^+ ions observed in the experiments reported here at moderate pressures of helium buffer gas are likely to be the result of intermolecular collisional stabilization of a relatively long-lived reaction intermediate. However, it should be noted that the contribution of bimolecular radiative association could not be evaluated since the total pressure of the ambient gas was not varied. In any case, all the association reactions observed with Si^+ were found to *compete* with bimolecular decomposition channels. In interstellar gas clouds radiative association which must compete with formation of bimolecular dissociation products can be argued to be unlikely.[26] On the other hand, the association reactions of silicon-containing molecular ions observed in our experiments which *do not compete* with bimolecular product channels may well proceed by radiative association in interstellar gas clouds. When followed by neutralization of the adduct ions, these reactions could then provide sources for more complex molecules. A number of such possibilities are indicated by our experiments. The kinds of molecules that may be formed are quite intriguing, as shown, for example, in the following reaction sequences

$$Si^+ \xrightarrow{HCN} CNSi^+ \xrightarrow{HCN} C_2HN_2Si^+ \xrightarrow{PT/e} :Si(CN)_2 \quad (21)$$

$$Si^+ \xrightarrow{HC_3N} C_2HSi^+ \xrightarrow{HC_3N} C_5H_2NSi^+ \xrightarrow{e} :Si(C_2H)C_3N \quad (22)$$

where PT and e refer to neutralization by proton transfer and recombination with electrons, respectively. Here substituted silenes are the neutral molecules which may ultimately be produced. The five-membered ring molecule given below is even a possible product in reaction 21. However, the true nature of the neutral products

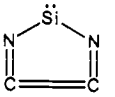

which may be formed in the final step in this chemistry is not known and remains to be explored and characterized.

Acknowledgment is made to the Natural Sciences and Engineering Research Council of Canada for the financial support of this research.

Registry No. Si^+, 14067-07-3; HCN, 74-90-8; C_2N_2, 460-19-5; CH_3CN, 75-05-8; HC_3N, 1070-71-9.

(26) Bates, D. R. *Astrophys. J.* **1983**, *267*, L121.

Pressure Dependence of the Electronic Spectra of Quasi-One-Dimensional Pt_2X Semiconductors

Mary Ann Stroud,[1a,b] Harry G. Drickamer,*[,1b] Miriam Heinrichs Zietlow,[1c] Harry B. Gray,*[,1c] and Basil I. Swanson*[,1a]

Contribution from the Isotope and Nuclear Chemistry Division, Los Alamos National Laboratory, Los Alamos, New Mexico 87545, School of Chemical Sciences, Department of Physics and Materials Research Laboratory, University of Illinois, Urbana, Illinois 61801, and No. 7766 from the Arthur Amos Noyes Laboratory, California Institute of Technology, Pasadena, California 91125. *Received May 5, 1988*

Abstract: The effects of high static pressure on the electronic absorption spectra of the mixed-valence semiconductors, $K_4[Pt_2(P_2O_5H_2)_4X]\cdot 3H_2O$ (X = Cl, Br), have been investigated to 10.0 GPa. Their electronic spectra exhibit bands attributable to the reduced complex, $[Bu_4N]_4[Pt_2(P_2O_5H_2)_4]$ ($d_{xz},d_{yz} \rightarrow p\sigma$, $d\sigma^* \rightarrow d_{x^2-y^2}$, and $d\sigma^* \rightarrow p\sigma$), and the oxidized complex, $K_4[Pt_2(P_2O_5H_2)_4X_2]\cdot 2H_2O$ ($d_{xz},d_{yz} \rightarrow d\sigma^*$ and $\sigma(X) \rightarrow d\sigma^*$), along with an intervalence charge-transfer (IVCT) band characteristic of a mixed-valence solid. The reduced (Pt_2) and oxidized (Pt_2X_2) complexes have also been studied so that direct comparisons with the monohalides (Pt_2X) could be made. The $\sigma(X) \rightarrow d\sigma^*$ transition (observed at 34 500, 32 800, and 35 400 cm^{-1} for Pt_2Cl_2, Pt_2Br, and Pt_2Cl, respectively) exhibits linear blue shifts of ca. 300 cm^{-1}/GPa for each complex. The $d\sigma^* \rightarrow d_{x^2-y^2}$ transition in Pt_2 (35 300 cm^{-1}) shifts red initially and then begins to shift blue above 5.5 GPa, while the $d\sigma^* \rightarrow p\sigma$ band (ca. 27 000 cm^{-1}) exhibits little shift with pressure for Pt_2, Pt_2Cl, and Pt_2Br. The dominant pressure-induced effects that give rise to the above shifts are (i) destabilization of the $d\sigma^*$ and $p\sigma$ levels through increased orbital overlap and d/p mixing and (ii) destabilization of the $d_{x^2-y^2}$ level at high pressure through increased ligand field interactions. The IVCT bands of Pt_2X exhibit strong red shifts with increasing pressure that are attributed to the movement of X in Pt_2X_2 toward Pt_2 in the linear chains that leads to an increase in the band character of the orbitals associated with this transition.

Quasi-one-dimensional, halide-bridged, mixed-valence, transition-metal complexes, MX, have been the focus of much recent research.[2-8] An important characteristic of these materials is that their physical properties may be controlled by varying the transition metal complex ions, the halogen, and external pressure. The materials exhibit an intense intervalence charge-transfer excitation, the IVCT band, that is polarized along the chain axis. Resonance

* Author to whom correspondence should be addressed.

(1) (a) INC-4, MS C346, University of California, Los Alamos National Laboratory. (b) School of Chemical Sciences, Department of Physics and Materials Research Laboratory. (c) Arthur Amos Noyes Laboratory, California Institute of Technology.

0002-7863/89/1511-0066$01.50/0

Raman spectra obtained by exciting into the IVCT band are also highly polarized along the chain axis and the frequencies of the Raman-enhanced modes have been used along with IVCT band energy as a measure of the extent of valence delocalization.[2c] These highly anisotropic semiconductors are generally in the trapped-valence limit, with the metal atoms in alternating valence states. These and similar systems have recently been recognized as examples of commensurate charge-density-wave (CDW) systems.[7,9,10] They exhibit a large distortion of the halogen from the central position between the metal dimers due to a Peierls instability.

Linear MMX chain complexes, $K_4[Pt_2(P_2O_5H_2)_4X]\cdot 3H_2O$, X = Cl, Br ($Pt_2X$), are of particular interest[11-15] because they are more valence delocalized and show smaller distortions of the halide sublattice relative to the MX systems. Early structural work on Pt_2Br indicated that the halogen was centrally located between the Pt dimers.[12] However, theoretical calculations suggested that there should be a distorted halide sublattice and some mixed-valence character.[14] Recent experimental studies have shown that there is a small distortion of the halogen from the central position in Pt_2Br.[11,15] In contrast, Pt_2Cl is in the strongly trapped-valence limit with a large distortion of the chloride from the central position.

Original interest in investigating these types of systems under high pressure was inspired by the research of Interrante and co-workers.[16] They investigated similar linear chain MX complexes and found that the conductivity could be increased by as much as nine orders of magnitude at 14.0 GPa, presumably because of a decrease in the Peierls distortion and the band gap with increasing pressure. This tremendous pressure dependence made these types of materials good candidates for spectroscopic studies. Tanino et al.[6] measured the effects of high pressure on the lattice parameters, optical gaps, luminescence peaks, and X-ray absorption near edge structure of MX complexes. It was concluded that the Peierls distortion decreases with increasing pressure. Results of a recent study on the pressure dependence of the Raman spectra of Pt_2Br are attributed to a reduction of the Peierls distortion, while Pt_2Cl resonance Raman studies indicate that the monochloride remains in a trapped-valence limit to 10.0 GPa.[17a,c]

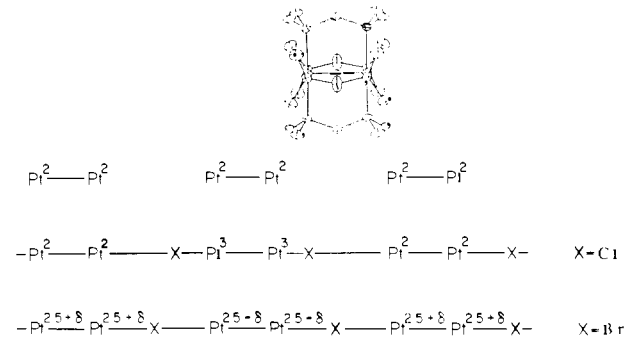

Figure 1. (a) ORTEP drawing of Pt_2. (b) Structures of Pt_2, Pt_2Cl, and Pt_2Br along the linear chain.

Table I. Ambient Pressure Energies of Electronic Transitions in cm^{-1}

transition	Pt_2Cl_2	Pt_2	Pt_2Br	Pt_2Cl
$d_{xz},d_{yz} \rightarrow d\sigma^*$	28 100			
$\sigma(X) \rightarrow d\sigma^*$	34 500		32 800	35 400
$d\sigma^* \rightarrow p\sigma$		26 700	27 600	26 400
$d_{xz},d_{yz} \rightarrow p\sigma$		40 200		
$d\sigma^* \rightarrow d_{x^2-y^2}$		35 300		
unassigned				25 600
IVCT			16 100	18 600

The effects of pressure on the electronic spectra of Pt_2Cl, Pt_2Br, $[Bu_4N]_4[Pt_2(P_2O_5H_2)_4](Pt_2)$, and $K_4[Pt_2(P_2O_5H_2)_4Cl_2]\cdot 2H_2O(Pt_2Cl_2)$ have been investigated in order to gain insight into the structural changes that can occur in these materials. The energy maximum of the IVCT band provides a direct diagnostic of the extent of valence delocalization in the monohalide complexes.[18] In addition, study of the other bands in the electronic spectra should yield valuable information on the effects of pressure on the electronic structures of the complexes. The magnitude and direction of the pressure-induced changes of the energy of the transitions provide information on changes in ligand field splitting and changes in the bond strength of the Pt-Pt complexes.

Experimental Apparatus and Procedures

Pressure was generated with use of a gasketed Merrill-Basset diamond anvil cell (DAC) with an inconel gasket. The high-energy working range of the cell was limited to 42 000 cm^{-1} because of the strong absorption by nitrogen impurities in the diamonds. A ruby fluorescence pressure calibration method was used to determine pressures. Absorption measurements were obtained at room temperature with a Perkin-Elmer 330 spectrophotometer. The instrument was modified for DAC work by using a 100-W tungsten-halogen lamp source and by adding a 5 to 1 beam condenser to the sample chamber.[19]

Fluorescence measurements were obtained on a SPEX Model 1403 $^3/_4$-m double monochromator equipped with a Princeton Applied Research photon counting system. Typically, the 514.5-nm line of a Spectra-Physics 171 argon laser was used as the exciting line. The cell was allowed to equilibrate after each pressure increase and ruby fluorescence was routinely checked before and after the data collection to ensure that the pressure had not varied significantly. When possible, the fluorescence from several rubies located in different parts of the cell was measured. Pressure gradients of as large as 0.4 GPa were observed at high pressures. Because of problems with sample degradation, the laser power at the sample was kept to less than 20 mW. For Pt_2Cl_2, Pt_2, and Pt_2Br, all pressure effects were reversible. Preliminary high-pressure investigations of $K_4[Pt_2(P_2O_5H_2)_4]\cdot 2H_2O$ and $K_4[Pt_2(P_2O_5H_2)_4Br_2]\cdot 3H_2O$ indicate irreversible effects occur with pressure. Degradation of the Pt_2Cl sample was a problem. Peak positions were always reversible; however, intensity changes and weak additional features in the release spectra were observed when sample degradation had occurred.

(2) (a) Clark, R. J. H. *Ann. N.Y. Acad. Sci.* **1978**, *313*, 672. (b) Keller, H. J. *Extended Linear Chain Compounds*; Miller, J. S., Ed.; Plenum: New York, 1982; p 357. (c) Clark, R. J. H. *Advances in Infrared and Raman Spectroscopy*; Clark, R. J. H., Hester, R. E. Eds.; Wiley: Heyden, 1984; vol. 11, p 95. (d) Clark, R. J. H. *Mixed Valence Compounds*; Brown, D. B., Ed.; Reidel: Dordrecht, 1982; p 271.

(3) Clark, R. J. H.; Kurmoo, M. *J. Chem. Soc., Faraday Trans.* **1983**, *79*, 519.

(4) Tanaka, M.; Kurita, V. *J. Phys. C: Solid State Phys.* **1986**, *19*, 3019.

(5) Conradson, S. D.; Dallinger, R. F.; Swanson, B. I.; Clark, R. J. H.; Croud, V. B. *Chem. Phys. Lett.* **1987**, *135*, 463.

(6) (a) Tanino, H.; Koshizuka, N.; Hoh, K.; Kato, K.; Yamashita, M.; Kobayashi, K. *Physica* **1986**, *39*, *140B*, 487. (b) Tanino, H.; Kobayshi, K; Yamashita, M. *Solid State Physics under Pressure*; Minomura, S., Ed.; KTK Scientific Publ. Co.: Tokyo, Japan, 1985; pp 115. (c) Tanino, H.; Koshizuka, N.; Kobayashi, K.; Yamashita, M.; Hoh, K. *J. Phys. Soc. Jpn.* **1985**, *54*, 483.

(7) (a) Baeriswyl, D.; Bishop, A. R. *J. Phys. C* **1988**, *21*, 339. (b) Baeriswyl, D.; Bishop, A. R. *Phys. Scr.* **1987**, *T19*, 239.

(8) (a) Tanaka, M.; Kurita, S.; Kojima, T.; Yamada, Y. *Chem. Phys.* **1984**, *91*, 257. (b) Tanaka, M.; Kurita, S. *J. Phys. C: Solid State Phys.* **1986**, *19*, 3019 and references therein.

(9) Ueta, M.; Kanzaki, H.; Kobayashi, K.; Toyozawa, Y.; Hanamura, E. *Excitonic Processes in Solids*; Berlin, 1986; Vol. 60, Chapter 9, Springer Series in Solid State Sciences.

(10) Onodera, Y. *J. Phys. Soc. Jpn.* **1987**, *56*, 250.

(11) Kurmoo, M.; Clark, R. J. H. *Inorg. Chem.* **1985**, *24*, 4420.

(12) Che, C.-M.; Herbstein, F. H.; Schaefer, W. P.; Marsh, R. E.; Gray, H. B. *J. Am. Chem. Soc.* **1983**, *105*, 4604.

(13) Conradson, S. D.; Stroud, M. A.; Zietlow, M. H.; Swanson, B. I.; Baeriswyl, D.; Bishop, A. R. *International Centre for Theoretical Physics* **1987**, IC/87/315; *Solid State Commun.* **1988**, *65*, 723.

(14) Whangbo, M.-H.; Canadell, E. *Inorg. Chem.* **1986**, *25*, 1726.

(15) Butler, L. G.; Zietlow, M. H.; Che, C.-M.; Schaefer, W. P.; Sridhar, S.; Grunthaner, P. J.; Swanson, B. I.; Clark, R. J. H.; Gray, H. B. *J. Am. Chem. Soc.* **1988**, *110*, 1155.

(16) Interrante, L. V.; Browall, K. W.; Bundy, F. P. *Inorg. Chem.* **1974**, *13*, 1158.

(17) (a) Stroud; M. A.; Swanson, B. I., manuscript in preparation. (b) See IVCT section of this article. (c) Swanson, B. I.; Stroud, M. A.; Conradson, S. D.; Zietlow, M. H. *Solid State Commun.* **1988**, *65*, 1405.

(18) Clark, R. J. H. *Chem. Soc. Rev.* **1984**, *13*, 219.

(19) The glitches that occurred in some of the electronic spectra at approximately 30 000 and 28 000 cm^{-1} were caused by the lamp change. The glitch at approximately 21 000 cm^{-1} was caused by a grating anomaly.

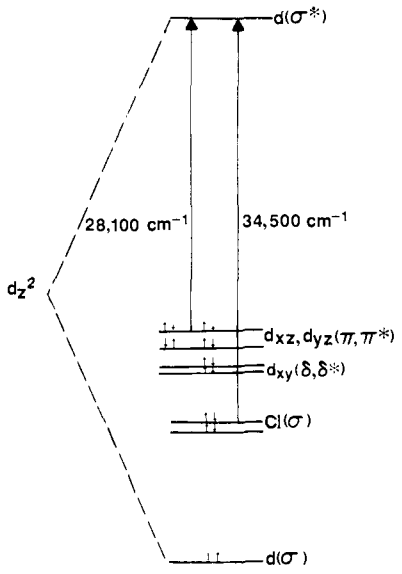

Figure 2. Energy level diagram for Pt_2Cl_2 at ambient pressure.

The complexes were prepared by published procedures.[12,15,20,21] For Pt_2Cl_2, a 3–5% mixture of Pt_2Cl_2 in $KClO_4$ was prepared and mixed for several minutes in a dental amalgamator. The sample was loaded into the cell immediately after mixing. Pressure was applied to the sample until the salt fused and the sample became transparent. The cell was released to zero pressure before the run was started. The Pt_2 crystals were ground in mineral oil under flowing N_2. When the crystals were ground in air, the electronic absorption spectra suggested that the sample was reacting. Samples prepared by minimal grinding of Pt_2Br single crystals with $KClO_4$ in a mortar and pestle resulted in the best obtainable electronic spectra. Single crystals of Pt_2Cl were ground in air and under flowing N_2. Mineral oil or $KClO_4$ was used as the pressurizing medium.

Sample-dependent high-energy scattering was observed in the electronic spectra. After correction for this scattering tail had been made, peak locations were determined with a cursor. Polynomial fits of all the energy vs pressure electronic data were determined. For many of the electronic transitions, the ambient-pressure peak locations were somewhat dependent on the sample preparation, through the pressure-induced shifts were not. Most likely, the major cause of these differences was varying particle size. In order to compare the relative pressure-induced shift of the energy of a transition in the different runs, an energy correction factor was subtracted from each run. The correction factor, ν_0, was determined by minimizing the standard deviation of a polynomial fit to the data. Wherever a significant energy difference resulted between runs, the ν_0 values are noted.

Results and Discussion

Pt_2, Pt_2Cl_2, Pt_2Cl, and Pt_2Br contain D_{4h} Pt_2P_8 units built by four binucleating pyrophosphite ligands, $[(HO_2P)_2O^{2-}]$ (Figure 1a). The potassium salts of the fully reduced complex and the monohalides (Pt_2Cl and Pt_2Br) are isostructural with the metal–metal bond aligned along the z axis of the tetragonal unit cell, $P4/mbm$, as illustrated in Figure 1b. In the monohalides, the Pt_2 units form an infinite linear chain in the z direction. The larger the distortion of the halogen from the central position, the larger the trapped-valence character of the chain. In Pt_2Cl, which is in the trapped-valence limit, the halogen is displaced 0.25 Å from the central position at 22 K[15] and the charge on the alternating Pt dimers is close to Pt(II)–Pt(II) and Pt(III)–Pt(III). In the more delocalized Pt_2Br complex, the halogen is displaced only 0.1 Å from the central position at 19 K,[15] and the charge on the Pt atoms is more delocalized. The ambient-pressure energies of all the electronic transitions studied as a function of pressure are listed in Table I.

Pt_2Cl_2. Two electronic transitions were studied as a function of pressure in Pt_2Cl_2, $d_{xz},d_{yz} \rightarrow d\sigma^*$ and $\sigma(X) \rightarrow d\sigma^*$ (Figure 2).[22]

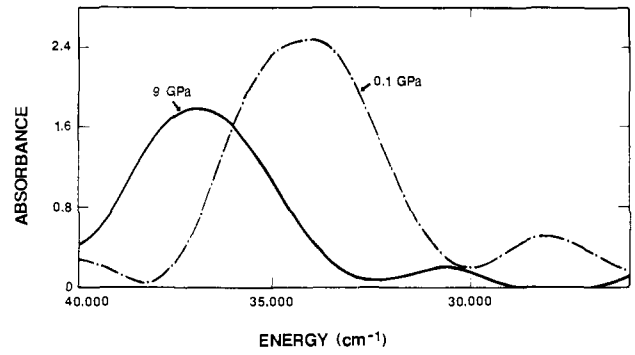

Figure 3. Absorption spectra of Pt_2Cl_2 at 0.1 and 9 GPa.

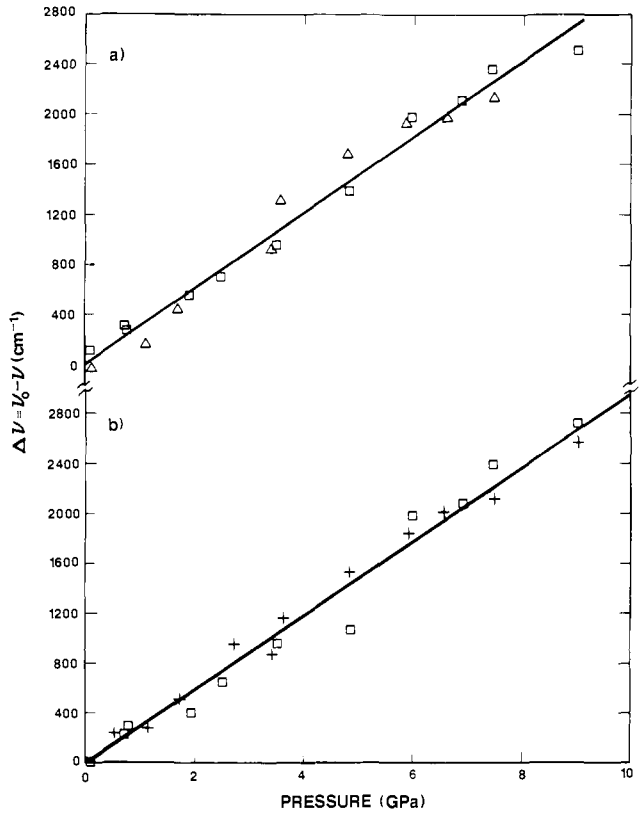

Figure 4. (a) Pressure shift of the $d_{xz},d_{yz} \rightarrow d\sigma^*$ transition in Pt_2Cl_2. (b) Pressure shift of the $\sigma(Cl) \rightarrow d\sigma^*$ transition in Pt_2Cl_2.

The $d\sigma \rightarrow d\sigma^*$ transition has been assigned to an absorption (at about 46 500 cm^{-1}) that is too high in energy to be observed in a diamond anvil cell. The smoothed absorption spectra of Pt_2Cl_2 at 0.1 and 9 GPa are shown in Figure 3.

The $d_{xz},d_{yz} \rightarrow d\sigma^*$ transition shifts blue with increasing pressure at a rate of 300 cm^{-1}/GPa from its position at 28 100 cm^{-1}. The shift is linear over the pressure range studied (Figure 4a). Increasing pressure enhances the overlap between the d_{z^2} orbitals on adjacent Pt atoms, thereby destabilizing $d\sigma^*$. Increased d_{z^2}–σ(Cl) interaction with increasing pressure would also destabilize $d\sigma^*$. The two sets of d_{xz},d_{yz} orbitals interact only weakly, so the shift of the $d_{xz},d_{yz} \rightarrow d\sigma^*$ transition is attributed to the pressure-induced destabilization of $d\sigma^*$. Any increase in the splitting of the d_{xz},d_{yz} orbitals would reduce the magnitude of the observed blue shift.

The energy of the $\sigma(Cl) \rightarrow d\sigma^*$ transition also blue shifts linearly, at a rate of 300 cm^{-1}/GPa from 34 500 cm^{-1} (Figure 4b). Accordingly, this blue shift is attributed mainly to the destabilization of $d\sigma^*$ with increasing pressure.

(20) Che, C.-M.; Schaefer, W. P.; Gray, H. B.; Dickson, M. K.; Stein, P. B.; Roundhill, D. M. *J. Am. Chem. Soc.* **1982**, *104*, 4253.
(21) Che, C.-M.; Butler, L. G.; Grunthaner, P. J.; Gray, H. B. *Inorg. Chem.* **1985**, *24*, 4662.
(22) Che, C.-M.; Mak, T. C.; Miskowski, V. M.; Gray, H. B. *J. Am. Chem. Soc.* **1986**, *108*, 7840.

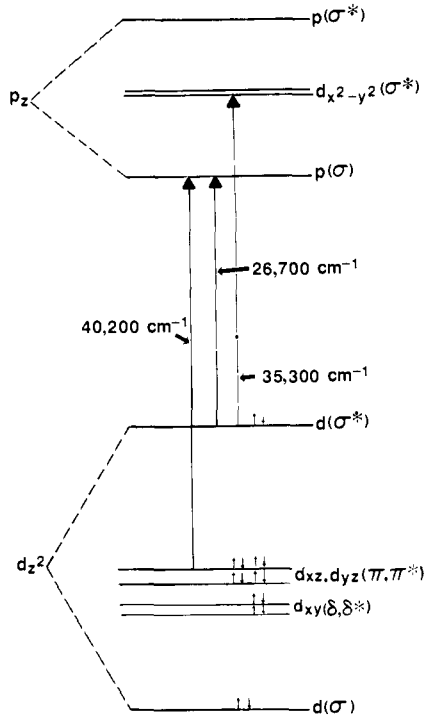

Figure 5. Energy level diagram for Pt_2 at ambient pressure.

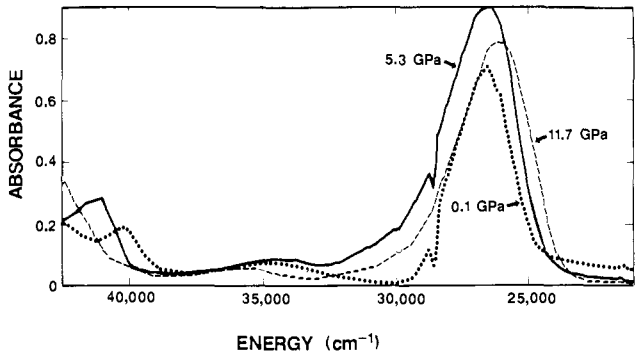

Figure 6. Absorption spectra of Pt_2 at 0.1, 5.2, and 11.7 GPa.

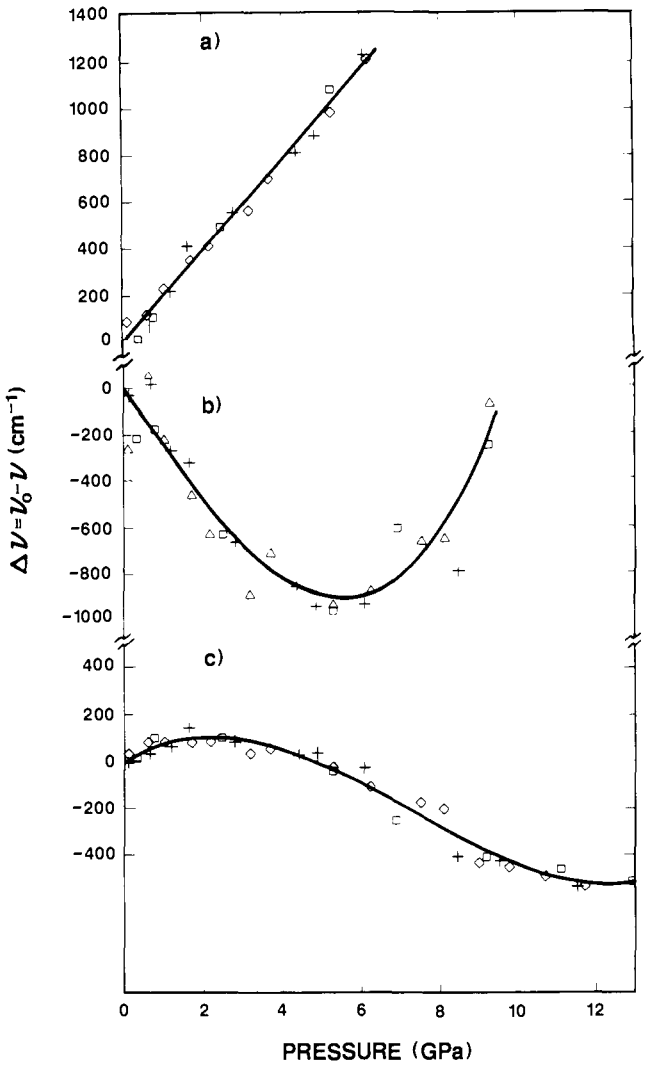

Figure 7. (a) Pressure shift of the $d_{xz},d_{yz} \rightarrow p\sigma$ transition in Pt_2. (b) Pressure shift of the $d\sigma^* \rightarrow d_{x^2-y^2}$ transition in Pt_2. (c) Pressure shift of the $d\sigma^* \rightarrow p\sigma$ transition in Pt_2.

Pt_2. The energy levels for the d^8–d^8 Pt_2 complex are illustrated in Figure 5. The effects of pressure on three electronic transitions, $d_{xz},d_{yz} \rightarrow p\sigma$, $d\sigma^* \rightarrow p\sigma$, and $d\sigma \rightarrow d_{x^2-y^2}$,[23] have been investigated (Figure 6).

The $d_{xz},d_{yz} \rightarrow p\sigma$ transition in Pt_2 (40 200 cm^{-1} at ambient pressure) exhibits a linear blue shift of 190 cm^{-1}/GPa with increasing pressure (Figure 7a). An explanation of the observed shift is that the p_z orbitals are coupled strongly to d_{z^2} orbitals on adjacent Pt atoms, while the d_{xz},d_{yz} orbitals experience only very weak π interactions. Destabilization of $d\sigma^*$ with increasing pressure (see below) therefore results in a destabilization of p_z relative to d_{xz},d_{yz}.

The $d\sigma^* \rightarrow d_{x^2-y^2}$ transition (ambient-pressure energy of 35 400 cm^{-1}) exhibits unusual nonlinear behavior with increasing pressure. The $d\sigma^* \rightarrow d_{x^2-y^2}$ transition shifts red up to 5.5 GPa at an initial rate of about 230 cm^{-1}/GPa and then levels off and begins to shift blue until at least 10.0 GPa (Figure 7b). This transition is expected to be affected both by increased splitting of $d\sigma$ and $d\sigma^*$, resulting from greater overlap of the d_{z^2} orbitals on adjacent Pt atoms, and an increased ligand field that destabilizes $d_{x^2-y^2}$ relative to d_{z^2}. In the absence of large changes in the ligand field splitting, an increase in the overlap of adjacent d_{z^2} orbitals would lead to a red shift, and it is reasonable that this is the dominant effect at low pressure. At higher pressures, increased ligand field splitting between $d_{x^2-y^2}$ and d_{z^2} begins to dominate and the $d\sigma^* \rightarrow d_{x^2-y^2}$ transition shifts to the blue. The strong nonlinearity of the ligand field effect is attributed to nonlinear compression of the P–Pt bonds as the pressure is increased. At low pressure, compression along the a and b crystallographic axes results in compression of the interchain separation and little or no change in the P–Pt bonds. At higher pressure, as the interchain interactions stiffen, the P–Pt bonds begin to compress, resulting in the destabilization of $d_{x^2-y^2}$.

There is little shift in the 26 700-cm^{-1} energy of $d\sigma^* \rightarrow p\sigma$ up to 5.0 GPa, though the transition does appear to initially shift slightly to the blue. At higher pressures, a significant red shift is observed; this shift appears to level off at ca. 11.0 GPa. Increased splitting of $d\sigma$ and $d\sigma^*$ would result in a red shift of the $d\sigma^* \rightarrow p\sigma$ transition. The $d\sigma^*$ and $p\sigma$ levels are coupled, and any increase in the coupling as the pressure is raised would tend to repel $d\sigma^*$ and $p\sigma$, resulting in a blue shift. For the $d\sigma^* \rightarrow p\sigma$ transition, there is probably a delicate balance between these two effects. Because a weak shift is observed, other effects also may significantly influence the behavior of this transition. At higher pressures, when the transition begins to red shift, increased coupling between the phosphorus σ orbital and $d\sigma^*$ occurs. Increased σ(P)–d_{z^2} coupling is expected at higher pressures in light of the observed pressure shift of the $d\sigma^* \rightarrow d_{x^2-y^2}$ transition. This effect suggests that the energy of the $d\sigma^*$ orbital may be tuned in binuclear complexes by varying the bridging ligand. For monohalide complexes, the ligands may be used to control the extent of delocalization of the chain.

The weak 22 000 cm^{-1} absorption attributable to the triplet $d\sigma^* \rightarrow p\sigma$ transition[23] initially shifts weakly blue with increasing

(23) Stiegman, A. E.; Rice, S. F.; Gray, H. B.; Miskowski, V. M. *Inorg. Chem.* **1987**, *26*, 1112.

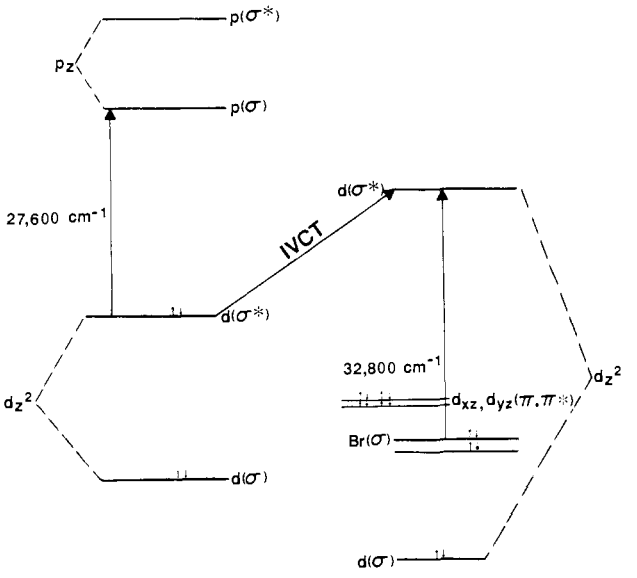

Figure 8. Energy level diagram for Pt_2Br at ambient pressure.

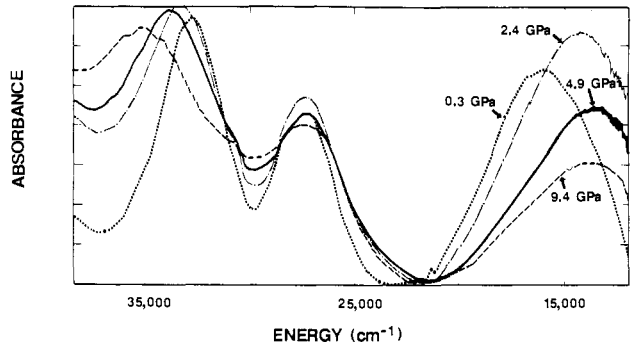

Figure 9. Absorption spectra of Pt_2Br at 0.3, 2.4, 4.9, and 9.4 GPa.

pressure. The weak 31 800-cm^{-1} shoulder is probably the $d\sigma^* \rightarrow d_{x^2-y^2}$ triplet,[23] which shifts red with increasing pressure.

Pt_2Br. A diagram of the electronic transitions in Pt_2Br is shown in Figure 8. The absorption spectrum of Pt_2Br is a superposition of electronic transitions in Pt_2 and Pt_2Br_2, modified slightly depending on the degree of delocalization, and an additional broad low-energy band, which is the IVCT characteristic of the mixed-valence complex itself (Figure 9). The highest energy transition observed in this study, 32 800 cm^{-1} at ambient pressure, shifts to higher energy with increasing pressure at a rate of 270 cm^{-1}/GPa (Figure 10a). The rate of the shift is within 10% of the observed shift of the $\sigma(Cl) \rightarrow d\sigma^*$ transition in Pt_2Cl_2 and it is linear over the pressure range studied. The band position at ambient pressure is very close to that of $\sigma(Br) \rightarrow d\sigma^*$ in Pt_2Br_2 (32 800 cm^{-1}),[20,24] and the absorption is intense. On the basis of this evidence, the band is assigned to the $\sigma(Br) \rightarrow d\sigma^*$ transition.

The pressure-induced energy change of the 27 600 cm^{-1} transition is shown in Figure 10b. The energy of the transition shifts weakly to the red with increasing pressure and appears to level off above 5.0 GPa. On the basis of our analysis of the Pt_2Cl_2 and Pt_2 results, a red shift of $d\sigma^* \rightarrow p\sigma$ is plausible, while a blue shift is expected for $d_{xz},d_{yz} \rightarrow d\sigma^*$. In Pt_2Br, a red shift of $d\sigma^* \rightarrow p\sigma$ also is expected at high pressure, because of enhanced intermolecular interactions along the metal–metal axis.[14] Accordingly, the intense 27 600 cm^{-1} band is assigned to $d\sigma^* \rightarrow p\sigma$.

Pt_2Cl. The energy level diagram for Pt_2Br (Figure 8) can also be utilized in discussing the spectrum of Pt_2Cl, where four electronic transitions have been studied as a function of pressure (Figure 11). The highest energy transition observed for Pt_2Cl (35 400 cm^{-1} at ambient pressure) shifts to higher energy with increasing pressure at a rate of 290 cm^{-1}/GPa (Figure 12a). The

(24) Isci, H.; Mason, W. R. *Inorg. Chem.* **1985**, *24*, 1761.

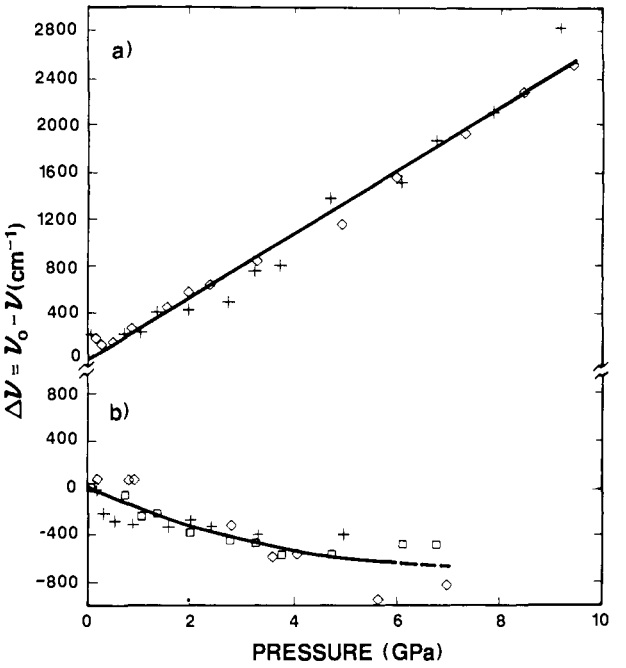

Figure 10. (a) Pressure shift of the $\sigma(Br) \rightarrow d\sigma^*$ transition in Pt_2Br. (b) Pressure shift of the $d\sigma^* \rightarrow p\sigma$ transition in Pt_2Br (ν_0 = 27 200, 27 600, and 27 900 cm^{-1}).

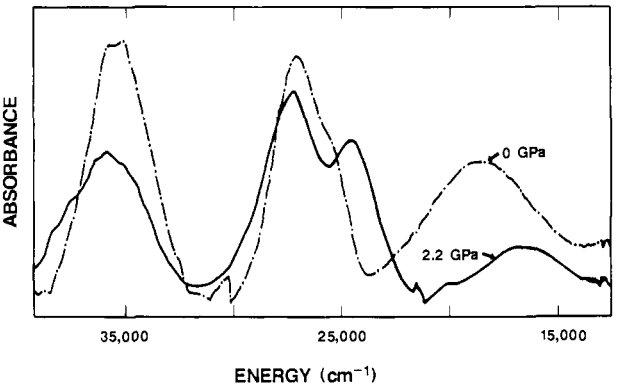

Figure 11. Absorption spectra of Pt_2Cl at ambient pressure (0) and 2.2 GPa.

shift is linear with pressure and its magnitude is within 10% of the observed shift of the $\sigma(Cl) \rightarrow d\sigma^*$ transition in Pt_2Cl_2. The energy of the transition at ambient pressure is close to that of $\sigma(Cl) \rightarrow d\sigma^*$ in Pt_2Cl_2 (Table I). Since the transition is also very intense, it is assigned to $\sigma(Cl) \rightarrow d\sigma^*$.

The weak blue shift, 75 cm^{-1}/GPa, of the transition at 26 700 cm^{-1} is illustrated in Figure 12b. A blue shift of the $d_{xz},d_{yz} \rightarrow d\sigma$ band has been observed in Pt_2Cl_2 and a similar shift of the energy level spacing can be inferred in Pt_2 by taking the difference between the pressure-induced shift of $d_{xz},d_{yz} \rightarrow p\sigma$ and that of $d\sigma^* \rightarrow p\sigma$; however, the shifts in Pt_2Cl_2 and Pt_2 are over twice that of the blue shift observed for the 26 700-cm^{-1} transition in Pt_2Cl. A blue shift is also plausible for $d\sigma^* \rightarrow p\sigma$ if and increase in the coupling between $d\sigma^*$ and $p\sigma$ is the dominant pressure effect. Accordingly, the intense 26 700 cm^{-1} band is assigned to the $d\sigma^* \rightarrow p\sigma$ transition.

There is a very strong pressure-induced linear red shift (−510 cm^{-1}/GPa) of the Pt_2Cl electronic transition with an ambient-pressure energy of 25 600 cm^{-1}. A weak red shift of the $d\sigma^* \rightarrow p\sigma$ transition has been observed for Pt_2Br and at pressures greater than 5.0 GPa for Pt_2. The magnitude of the red shift of the 25 600 cm^{-1} band is several times larger and for this reason assignment to $d\sigma^* \rightarrow p\sigma$ is unlikely. (In addition, the 26 700 cm^{-1} band has already been assigned to the $d\sigma^* \rightarrow p\sigma$ transition.) Another unusual characteristic of this transition is that the intensity of the

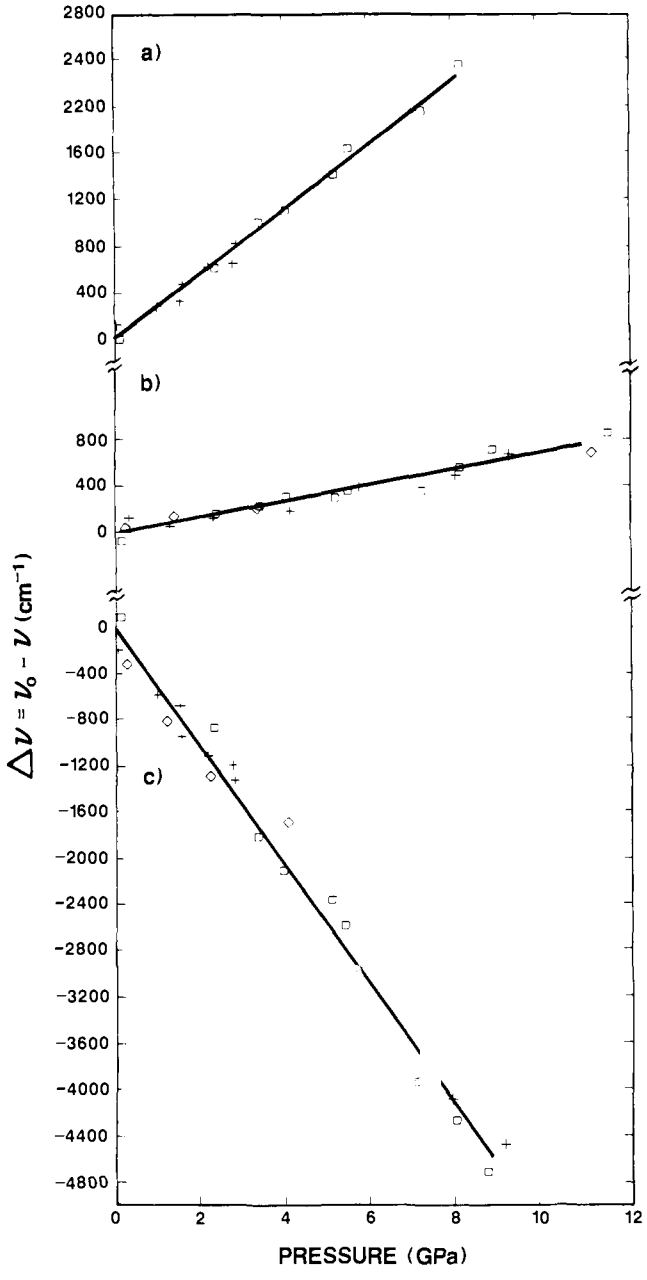

Figure 12. (a) Pressure shift of the σ(Cl) → dσ* transition in Pt_2Cl. (b) Pressure shift of the dσ* → pσ transition in Pt_2Cl (ν_0 = 26 200, 26 800, and 27 100 cm^{-1}). (c) Pressure shift of the unassigned transition in Pt_2Cl.

peak varies considerably with the method of sample preparation. The peak has been observed previously in the electronic spectra of samples in $KClO_4$ pellets,[11] and there is no peak in the Pt_2Br electronic spectrum that exhibits similar behavior. Because of these observations, the peak has not been assigned to a metal-based transition of the ground-state structure. The transition may result from a defect state present in the crystal. Resonance Raman spectra of Pt_2Cl show evidence for fine structure that grows in when the excitation wavelength is tuned to the red of the IVCT band. This fine structure was attributed to a polaronic local state resulting from a deficiency of K^+ ions.[13] On the basis of the Peierls-Hubbard 3/4 filled 2-band model developed by Baeriswyl and Bishop,[7] the energies of the defect electronic transitions are predicted to be to the blue as well as to the red of the IVCT band.

Intervalence Charge-Transfer Excitation. In the limit of a strongly trapped-valence material with a large distortion of the halogen from the central position, the IVCT band corresponds to dσ* → dσ* electron transfer along the chain axis from Pt_2 to an adjacent Pt_2X_2 (Figure 8). The energy of the IVCT band at ambient pressure in the trapped-valence Pt_2Cl complex is 18 600 cm^{-1}; it is significantly lower (16 100 cm^{-1}) in the more delocalized Pt_2Br complex. The lower the energy of the IVCT band, the more delocalized the complex.[18]) In Pt_2Cl and Pt_2Br, as the pressure increases, the IVCT band initially shifts strongly to lower energy and then appears to level off above 4.0 GPa (Figure 13). The initial red shift is approximately −750 cm^{-1}/GPa in Pt_2Cl and −1000 cm^{-1}/GPa in Pt_2Br. By way of comparison, the absorption edge of Wolfram's red salt shifts to lower energy at a rate of −1600 cm^{-1}/GPa up to 3.4 GPa.[6c]

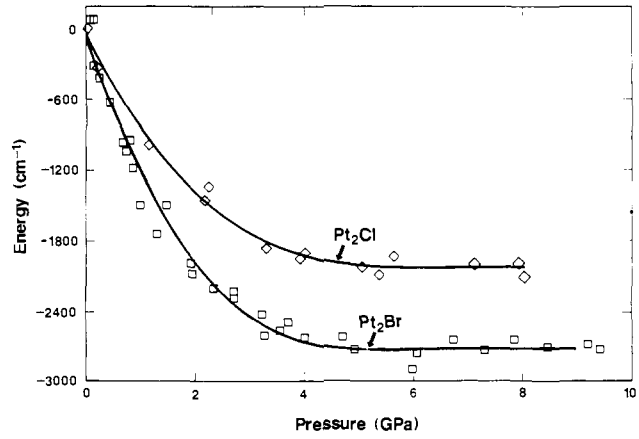

Figure 13. Relative energy shifts of the IVCT bands in Pt_2Br (ν_0 = 15 700, 16 200, and 16 400 cm^{-1}) and Pt_2Cl (ν_0 = 18 400, 18 500, and 18 900 cm^{-1}).

The strong red shift of the IVCT band with increasing pressure is consistent with a continuous change toward a symmetric structure with the halogen located equidistant between adjacent Pt dimers. As the halogen becomes more centrally located, there will be a decrease in the energy difference between dσ* orbitals on adjacent Pt dimers. The red shift of the IVCT band will be further enhanced by a decrease in the halide distortion, because the extent of delocalization along the z axis will increase the band character of the dσ* orbitals. Band calculation by Whangbo and Canadell on a related MMX system supports these conclusions.[14] The leveling observed at higher pressure may result from an increase in the electronic coupling between adjacent Pt dimers.[25a]

In interpreting pressure-induced changes of the IVCT band, it is important to separate the effects of structural changes from those of changes in orbital overlap. In this case, we can establish an upper limit to the red shift caused by increasing overlap by comparing the shifts of the IVCT bands in Pt_2Cl and Pt_2Br. The red shift observed for the IVCT band in Pt_2Br is 4/3 times as large as that observed for Pt_2Cl. Accordingly, at least the increased red shift of the IVCT band in Pt_2Br is attributed to the movement of the Br atom toward the center position relative to the surrounding Pt_2 fragments.

Comparisons of Pt_2Cl_2, Pt_2, and Pt_2X Transitions

A pressure-induced blue shift of the d_{xz},d_{yz} → dσ* transition in Pt_2Cl_2 of approximately 300 cm^{-1}/GPa was observed and a shift of 190 cm^{-1}/GPa can be inferred for Pt_2. It is reasonable for the dσ* orbital in Pt_2Cl_2 to be destabilized more rapidly than in Pt_2 because it is coupled to the halogen orbitals. By way of comparison, the $Mn_2(CO)_{10}$ d_{xz},d_{yz} → dσ* transition blue shifts at an initial rate of 500 cm^{-1}/GPa in the solid state.[26] However, the pressure-induced shift of the transition in $Mn_2(CO)_{10}$ is influenced by stabilization of the dπ levels because of increased π-back-bonding with the carbonyl ligands.

The pressure-induced shifts of the dσ* → pσ transition in Pt_2, Pt_2Br, and Pt_2Cl are compared in Figure 14. A weak shift was observed in all three complexes; however, the direction of the shift

(25) (a) Piepho, S. B.; Krausz, E. R.; Schatz, P. N. *J. Am. Chem. Soc.* **1978**, *100*, 2996. Hammack, W. S.; Lowery, M. D.; Hendrickson, D. N.; Drickamer, H. G. *J. Am. Chem. Soc.* **1987**, *109*, 7340.

(26) Carroll, T. L.; Shapley, J. R.; Drickamer, H. G. *Chem. Phys. Lett.* **1985**, *119*, 340.

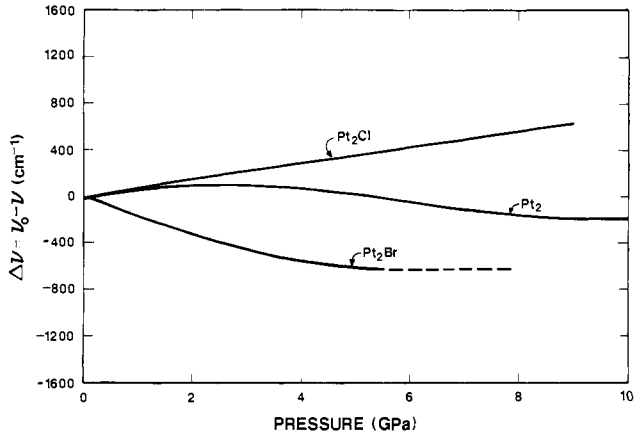

Figure 14. Relative energy shifts of the $d\sigma^* \rightarrow p\sigma$ transition in Pt_2Cl, Pt_2, and Pt_2Br.

varies, thereby indicating that there is a delicate balance among several competing effects. Increased coupling between the d_{z^2} and p_z orbitals, which may be somewhat larger in the monohalides because of the presence of the bridging halide, blue shifts $d\sigma^* \rightarrow p\sigma$. This appears to be the dominant effect in Pt_2Cl. The observed red shift in Pt_2Br can be explained in terms of band broadening of the $d\sigma^*$ and $p\sigma$ orbitals due to enhanced intermolecular interactions along the z axis. The band broadening should be larger in Pt_2Br than in Pt_2Cl, since Pt_2Br becomes delocalized more rapidly with increasing pressure.[17] A red shift of the $d\sigma^* \rightarrow p\sigma$ transition also results from an increase in the coupling of $d\sigma^*$ with the phosphorus σ orbitals, an effect that becomes important in Pt_2 at high pressure.

Acknowledgment. We acknowledge helpful discussions with Drs. Stephen F. Agnew, P. Jeffrey Hay, and Vincent M. Miskowski. M.A.S. thanks Dr. Agnew, Dr. Phillip D. Stroud, and Douglas G. Eckhart for technical assistance. This work was supported in part by the Center for Materials Science at Los Alamos National Laboratory. This work was performed under the auspices of the U.S. Department of Energy and was partially supported by the Materials Science Division under contract DE-AC02-76ER01198. Research at the California Institute of Technology was supported by the National Science Foundation (CHE8419828).

Registry No. Pt_2Cl, 99632-89-0; Pt_2Br, 85553-24-8; Pt_2, 89462-52-2; Pt_2Cl_2, 82135-56-6.

$[HNCO]^{\cdot+}$, $[HCNO]^{\cdot+}$, and $[CNOH]^{\cdot+}$ and Their Neutral Counterparts Studied by Mass Spectrometry[1]

Cornelis E. C. A. Hop,[†] Klaas-Jan van den Berg,[§] John L. Holmes,*[,†] and Johan K. Terlouw*[,§]

Contribution from the Analytical Chemistry Laboratory, University of Utrecht, Croesestraat 77a, Utrecht 3522 AD, The Netherlands, and the Department of Chemistry, University of Ottawa, Ottawa, Ontario K1N 6N5, Canada. *Received May 18, 1988*

Abstract: The isomeric ions $[HNCO]^{\cdot+}$, $[HCNO]^{\cdot+}$, and $[CNOH]^{\cdot+}$ have been generated and characterized in the gas phase by mass spectrometry. The neutralization–reionization technique was used to identify their neutral counterparts as stable species in the gas phase. The ions and their neutral counterparts were not observed to isomerize or tautomerize.

In 1826 the first experimental evidence was presented for isomerism, a concept earlier put forward by Berzelius; Liebig and Wöhler, after long debate, reached agreement that fulminic acid, HCNO, and isocyanic acid, HNCO, have the same elementary composition but are structurally distinct.[2]

It was long believed that isocyanic acid, HNCO, and cyanic acid, NCOH, were in tautomeric equilibrium with the hydroxy form prevailing. During the period of 1935–1950 it was established, mainly from spectroscopic evidence, that the free acid exists exclusively as HNCO.[3] Spectroscopy[4] also showed that gaseous fulminic acid has exclusively the HCNO structure and not, as proposed by Nef in 1894,[5] the tautomeric CNOH structure. Although cyanic acid, NCOH, could be produced by photolysis of isocyanic acid in an argon matrix at 4 K,[6a] similar experiments with fulminic acid failed to produce isofulminic acid, CNOH.[6b]

Because of their historic importance and their possible participation in interstellar chemistry, these four [H, C, N, O] isomers have received considerable attention from theoreticians.[7] From recent ab intio molecular orbital theory calculations[7b] it was concluded that all four isomers are stable and that high energy barriers prevent their interconversion. HNCO was the most stable isomer; its experimental heat of formation, $\Delta H_f°$, is ca. −105 kJ·mol^{-1}.[8] By using the calculated relative energies, $\Delta H_f°$(NCOH) = −17 kJ·mol^{-1}, $\Delta H_f°$(HCNO) = 228 kJ·mol^{-1}, and $\Delta H_f°$(CNOH) = 235 kJ·mol^{-1}. In spite of their predicted stability, NCOH and CNOH have eluded observation in the gas phase.

No calculations are available for the four radical cations, and experimental results[9] have been limited. For HNCO its photo-

§ University of Utrecht.
† University of Ottawa.

(1) A preliminary report recently appeared: Hop, C. E. C. A.; Holmes, J. L.; Van den Berg, K. J.; Terlouw, J. K. *Rapid Commun. Mass Spectrom.* **1987**, *1*, 52.
(2) (a) Liebig, J. *Ann. Chim. Phys.* [2] **1823**, *24*, 294. (b) Wöhler, F. *Ann. Chim. Phys.* [2] **1824**, *27*, 196. (c) Liebig, J. *Schweiggers Jahrbuch der Chemie und Physik* **1826**, *18*, 376.
(3) *Gmelin Handbuch der anorganischen Chemie*, 8th ed.; Verlag Chemie GmBH: Weinheim, 1971; Vol 14C [D1].
(4) (a) Beck, W.; Feldl, K. *Angew. Chem., Int. Ed. Engl.* **1966**, *5*, 722. (b) Beck, W.; Swoboda, P.; Feldl, K.; Tobias, R. S. *Chem. Ber.* **1971**, *104*, 533.
(5) Nef, J. U. *Liebigs Ann. Chem.* **1894**, *280*, 291.
(6) (a) Jacox, M. E.; Milligan, D. E. *J. Chem. Phys.* **1964**, *40*, 2457. (b) Bondybey, V E.; English, J. H.; Weldon Mathews, C.; Contolini, R. J. *J. Mol. Spectrosc.* **1982**, *92*, 431.
(7) (a) Pauling, L.; Hendricks, S. B. *J. Am. Chem. Soc.* **1926**, *48*, 641. (b) Poppinger, D.; Radom, L.; Pople, J. A. *J. Am. Chem. Soc.* **1977**, *99*, 7806. (c) McLean, A. D.; Loew, G. H.; Berkowitz, D. S. *J. Mol. Spectrosc.* **1977**, *64*, 184. (d) Rauk, A.; Alewood, P. F. *Can. J. Chem.* **1977**, *55*, 1498.
(8) Lias, S. G.; Bartmess, J. E.; Holmes, J. L.; Levin, R. D.; Liebman, J. F. *J. Phys. Chem. Ref. Data* **1988**, *17*, Suppl. 1.

0002-7863/89/1511-0072$01.50/0